Applied and Environmental Microbiology, Nov. 2008, p. 6774–6781 Vol. 74, No. 21
0099-2240/08/$08.00+0 doi:10.1128/AEM.01233-08
Copyright © 2008, American Society for Microbiology. All Rights Reserved.

Time-Lapse Microscopy of *Streptomyces coelicolor* Growth and Sporulation▽†

Vinod Jyothikumar, Emma J. Tilley, Rashmi Wali, and Paul R. Herron*

Strathclyde Institute of Pharmacy and Biomedical Science, University of Strathclyde, Royal College, 204 George Street, Glasgow G1 1 XW, United Kingdom

Received 3 June 2008/Accepted 25 August 2008

Bacteria from the genus *Streptomyces* are among the most complex of all prokaryotes; not only do they grow as a complex mycelium, they also differentiate to form aerial hyphae before developing further to form spore chains. This developmental heterogeneity of streptomycete microcolonies makes studying the dynamic processes that contribute to growth and development a challenging procedure. As a result, in order to study the mechanisms that underpin streptomycete growth, we have developed a system for studying hyphal extension, protein trafficking, and sporulation by time-lapse microscopy. Through the use of time-lapse microscopy we have demonstrated that *Streptomyces coelicolor* germ tubes undergo a temporary arrest in their growth when in close proximity to sibling extension sites. Following germination, in this system, hyphae extended at a rate of ~20 μm h^{-1}, which was not significantly different from the rate at which the apical ring of the cytokinetic protein FtsZ progressed along extending hyphae through a spiraling movement. Although we were able to generate movies for streptomycete sporulation, we were unable to do so for either the erection of aerial hyphae or the early stages of sporulation. Despite this, it was possible to demonstrate an arrest of aerial hyphal development that we suggest is through the depolymerization of FtsZ-enhanced green fluorescent protein (GFP). Consequently, the imaging system reported here provides a system that allows the dynamic movement of GFP-tagged proteins involved in growth and development of *S. coelicolor* to be tracked and their role in cytokinesis to be characterized during the streptomycete life cycle.

Fluorescence microscopy has revolutionized our understanding of the bacterial cell and provided new opportunities to investigate the behavior of cell division proteins and chromosome dynamics in bacteria (25). Central to this research is the application of time-lapse microscopy to study bacterial cell division, which has revealed the complexity with which bacteria coordinate cellular growth and division. For example, the rod-shaped bacteria *Escherichia coli* and *Bacillus subtilis* incorporate new peptidoglycan into their cell wall along their lateral walls, while coccoid bacteria such as *Staphylococcus aureus* do so at mid-cell (4). Actinobacteria, such as *Corynebacterium* and members of the mycelial, antibiotic-producing genus *Streptomyces*, incorporate peptidoglycan at the cell poles (4). In the case of streptomycetes, this allows them to adopt a hyphal growth strategy through peptidoglycan incorporation at the hyphal tip (9). This is ideally suited to the colonization of their particulate habitat, the soil, through the generation of a mycelium that permits nutrients to be transported from a nutrient reservoir to the actively growing tip. As such, streptomycetes represent a group of organisms that grow in a fashion distinct from other, better understood bacteria. The knowledge base associated with morphological and physiological differentiation in the model organism *Streptomyces coelicolor*, coupled with the viability of cell division mutants, means that a greater understanding of streptomycete growth and sporulation may provide important clues to understanding bacterial growth in general (18, 21). Perhaps one reason why an understanding of streptomycete cell division has lagged behind that for other bacteria is the technical difficulty associated with imaging this complex bacterium. To date, microscopic studies of cell division in streptomycetes have generated snapshot images of hyphae or spores. Such images can give only limited information on protein and nucleoid movement in space and time, and, as a result, the exact order of intracellular events during hyphal growth and sporulation in *Streptomyces* is still largely obscure (5, 6). The multinucleate nature of streptomycete hyphae means that time-lapse microscopy is likely to prove a key tool in understanding patterns in nucleoid and protein trafficking during hyphal growth, and although it was used to demonstrate spatial and temporal localization of cephamycin C biosynthesis in *Streptomyces clavuligerus* (11), so far it has not been used to study growth and development. Perhaps the main reasons for this are the technical challenges associated with carrying out time-lapse microscopy of the model organism, *S. coelicolor*. These include oxygen dependence, a developmentally heterogeneous mycelium, the three-dimensional pattern of hyphal growth, and an inability to sporulate in the absence of a solid support. Consequently, we set out to design an imaging system that could overcome at least some of these technical problems and support time-lapse microscopy of hyphal growth and sporulation. In order to do this, we exploited the design features of an inverted microscope coupled with rendering of three-dimensional representations of phase-contrast images and the availability of oxygen-permeable imaging chambers.

* Corresponding author. Mailing address: Strathclyde Institute of Pharmacy and Biomedical Science, University of Strathclyde, Royal College, 204 George Street, Glasgow G1 1 XW, United Kingdom. Phone: 44-141-5482531. Fax:. 44-141-5484924. E-mail: paul.herron@strath.ac.uk.

† Supplemental material for this article may be found at http://aem.asm.org/.

▽ Published ahead of print on 12 September 2008.

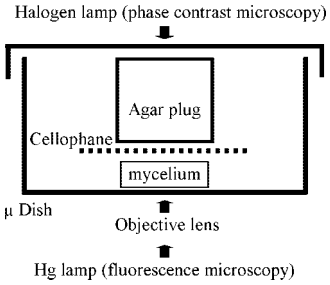

FIG. 1. Imaging chamber for capturing streptomycete growth on solid medium. Spores were germinated for an appropriate length of time on cellophane disks on agar before being inverted and transferred to the μ-dish imaging chamber. Subsequently, a cylinder of 3MA was applied to the cellophane dish and the imaging chamber transferred to the incubation chamber set to 30°C and allowed to equilibrate for 1 hour before commencement of imaging.

MATERIALS AND METHODS

Bacterial strains and cultivation conditions. *S. coelicolor* M145 and *S. coelicolor* K113 (a derivative of *S. coelicolor* M145 containing a second copy of *ftsZ* translationally fused to the enhanced green fluorescent protein [EGFP] gene [7]; generously supplied by Klas Flärdh, Lund University, Sweden) were grown on MS agar and supplemented with apramycin (100 μg ml^{-1}) when necessary at 30°C (16). For time-lapse microscopy, minimal agar (16) containing 5% (wt/vol) mannitol (3MA) or tap water agar (1% [wt/vol]) was used as circumstances required. For time-lapse microscopy of germination or growth of substrate hyphae, spores were germinated on 0.5-cm^2 sterile cellophane squares, placed on 3MA, and incubated at 30°C. Cellophane was removed after appropriate time intervals and transferred to imaging chambers. Time-lapse microscopy of sporulation was carried out by placing cellophane squares on sterile coverslips and inserting the coverslip into 3MA at an acute angle before inoculation with around 1×10^7 *S. coelicolor* spores (26). After 36 h, the cellophane was peeled away from the coverslip and transferred to imaging chambers.

Imaging chambers. Cellophane squares were placed, hyphal side down, in uncoated μ-dishes (Ibidi GmbH, Munich, Germany), and a plug of agar cut with a number 4 cork borer was placed on top of the cellophane. 3MA was used for germination or hyphal growth, and water agar was used for sporulation (Fig. 1). The microscope stage was heated to 30°C using an Ibidi heating system with a heated lid (Ibidi GmbH, Munich, Germany). In order to minimize focal drift, the microscope stage and imaging chamber were allowed to equilibrate for 60 min with respect to temperature before imaging commenced.

Fluorescence microscopy. Samples were studied using a Nikon TE2000S inverted microscope and observed with a CFI Plan Fluor DLL-100X oil N.A. 1.3 objective lens, and images were captured using a Hamamatsu Orca-285 Firewire digital charge-coupled device camera. Captured images were processed using IPlabs 3.7 image processing software (BD Biosciences Bioimaging, Rockville, MD). Briefly, 0.5-μm Z sections of both phase-contrast and fluorescent images were captured at 15-min intervals and used to render three-dimensional images. FtsZ-EGFP in *S. coelicolor* K113 was visualized with a fluorescein isothiocyanate filter set at an exposure time of 100 ms. Measurements of hyphal growth and Z-ring movement were made using IPlabs 3.7 image processing software and analyzed statistically using Microsoft Excel 2003; equality of variance between data sets was first determined using F tests and then subjected to the appropriate Student *t* test depending on the outcome of the F test. Multiple data sets were analyzed by analysis of variance. Where appropriate, means are supplemented by standard deviations in parentheses.

RESULTS

Germination of *S. coelicolor* M145 is heterogeneous and displays apical dominance. Although *S. coelicolor* is able to survive in the absence of oxygen for long periods of time (28), despite several attempts to grow *S. coelicolor* on agar sandwiched between glass coverslips and slides using a variety of imaging chambers, we were unable to do so. Presumably this was due to poor oxygen availability. As a result, we took advantage of the oxygen permeability and optically high quality of the plastic used in μ-dish manufacture in order to carry out time-lapse microscopy of hyphal growth. Spores of *S. coelicolor* M145 were inoculated onto a cellophane disk on 3MA, allowed to air dry for 30 min at 30°C, transferred to the imaging chamber (Fig. 1), and allowed to equilibrate for 1 hour before initiation of time-lapse microscopy. We analyzed the development of 90 spores individually. A total of 85% of spores swelled and became phase dark prior to germ tube emergence; this is characteristic of spore germination before germ tube emergence (27). A total of 15% of spores did not germinate, at least until hyphal growth made observation of individual spores difficult. It was impossible to describe accurately the germination pattern of 26% of the spores because of the difficulty of attributing individual hyphae to a parental spore due to spore clumping and hyphal overgrowth. However, we were able to track and describe the germination and early branching behavior of the remaining spores (59%). Emergence of a primary germ tube occurred between 2.25 and 6 h after initiation of imaging (3.75 and 7.5 h, respectively, after the original plating out), and 63.3% of spores produced one hypha and 36.7% produced two hyphae (Table 1). No spores that produced more than two hyphae were observed, in contrast to the results of Noens et al. (24), who observed as many as four germ tubes per spore.

Two classes of microcolonies developed in those spores that produced one germ tube: when a branch emerged from the primary germ tube, 7 (14.3%) primary germ tubes ceased growth for an average of 3.1 (±2.16) hours (Fig. 2A; see Movie S2A in the supplemental material), while the remaining 20 (49%) primary germ tubes showed no growth cessation (Fig. 2C; see Movie S2C in the supplemental material). Where growth of the primary germ tube was arrested, it was apparent that, following branch emergence, the branching occurred relatively soon after germination. Germ tubes that displayed growth arrest did so when a branch emerged on average 2.7

TABLE 1. Heterogeneity of *S. coelicolor* microcolonies following germination

Germination class[a]	No. of hyphae emerging from each spore	Growth arrest of primary hypha	% of germinations	$e_2 - e_1$[b] (h)	e_1 arrest[c] (h)
A	1	Yes	14.3	2.7 (1.45)	3.1 (2.16)
C	1	No	49.0	5.7 (1.62)	
B	2	Yes	20.4	1.4 (1.46)	4.9 (2.44)
D	2	No	16.3	3.5 (2.23)	

[a] Germination of a random selection of spores was observed by time-lapse microscopy, and four classes of spore germinations were observed: one or two hyphae, with or without growth arrest.

[b] Time difference between emergence of primary hypha at time e_1 from a spore and appearance of a second extension site at time e_2; the latter was the first hyphal branch (class A or C) or the emergence of a second hypha from the spore (class B or D). $e_2 - e_1$ values were compared statistically by the Student *t* test with respect to arrested (class A) and non arrested spores (class C) with one germ tube ($P < 1 \times 10^{-4}$), arrested (class B) and non arrested (class D) spores with two germ tubes ($P < 0.013$), arrested spores with one (class A) or two (class B) germ tubes ($P < 0.048$), and nonarrested germ tubes with one (class C) or two (class D) spores ($P < 0.004$). All four comparisons showed significant differences between the two populations in each individual test. Standard deviations are shown in parentheses.

[c] Time between cessation of growth of primary hypha and subsequent restart of growth. Standard deviations are shown in parentheses.

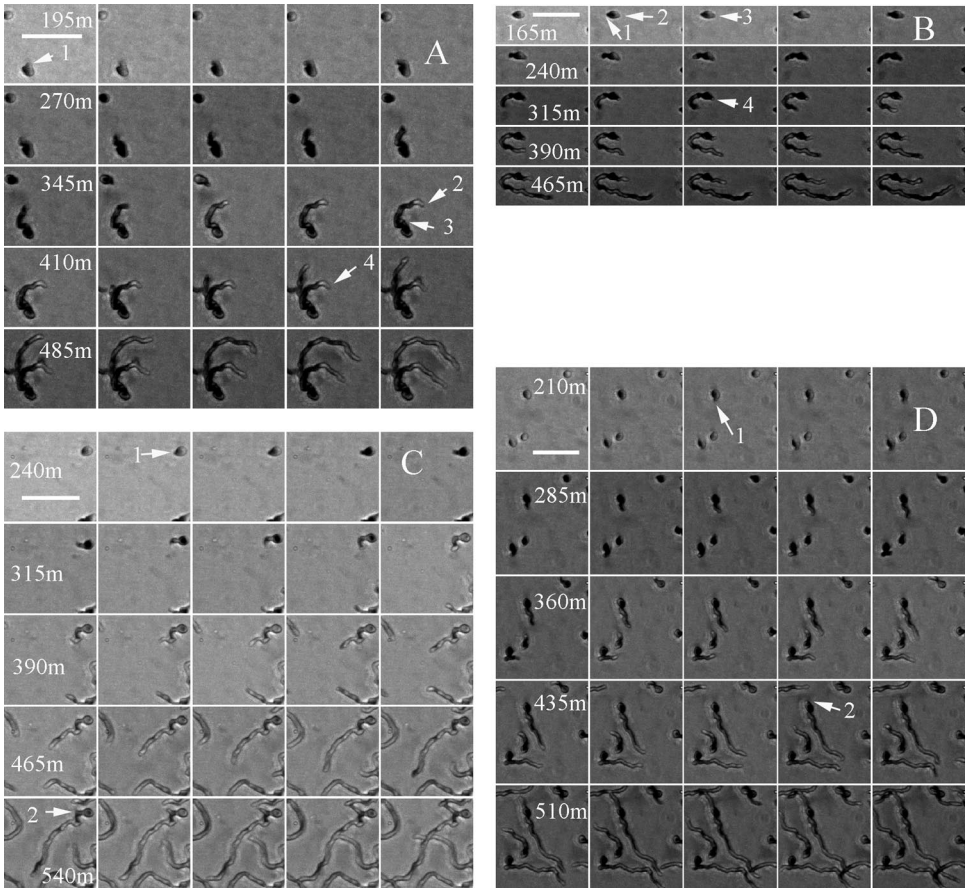

FIG. 2. Heterogeneity of *S. coelicolor* microcolonies following germination. Numbers represent minutes after initiation of time-lapse microscopy (see Movies S2A, S2B, S2C, and S2D in the supplemental material). Horizontal white bars represent 10 μm. The four observed classes of *S. coelicolor* germination are displayed. (A) Class A germination, showing emergence of the primary hypha (1), growth arrest of the primary hypha (2) following branch emergence (3), and growth restoration of the primary hypha (4). (B) Class B germination, showing two hyphae emerging from the spore (1 and 2), growth arrest by one hypha (3), and growth restoration of the arrested hypha (4). (C) Class C germination, showing hyphal emergence (1) and branch appearance (2) (no growth arrest of the primary hypha). (D) Class D germination, showing emergence of the primary hypha (1) and emergence of the secondary hypha (2) from the spore (no growth arrest of the primary hypha).

(±1.45) hours after germination, when the mean primary germ tube length was 2.3 μm, and these were termed class A germinations (Fig. 2A; see Movie S2A in the supplemental material). When no growth arrest was observed, the first branch emerged on average 5.7 (±1.62) hours after germination, when the mean primary germ tube length was 5.1 μm; these were termed class C germinations (Fig. 2C; see Movie S2C in the supplemental material). The time interval ($e_2 - e_1$) between the emergence of the first (germination) and the second (branch) growing tip was significantly longer in class C germinations than in class A germinations (Table 1).

Two classes of hyphal morphology were also generated from those spores that produced two germ tubes; 10 (20.4%) primary germ tubes ceased growth for an average of 4.9 (±2.44) hours following the emergence of a second germ tube from the same spore (Fig. 2B; see Movie S2B in the supplemental material). Meanwhile another eight primary germ tubes (16.3%) showed no growth arrest (Fig. 2D; see Movie S2D in the supplemental material). As was the case with branching in class A germinations, it was apparent that where growth of a primary germ tube was arrested following the emergence of a second germ tube, the latter occurred relatively soon after the primary germination. Primary germ tubes that displayed growth arrest did so when a second tube emerged on average 1.4 (±1.46) hours after germination; these were termed class B germinations (Fig. 2B; see Movie S2B in the supplemental material). Occasionally, two germ tubes emerged simultaneously from a spore; one always ceased growth for a period of time (Fig. 2B; see Movie S2A in the supplemental material). When no growth arrest was observed, the secondary germ tube emerged on average 3.5 (±2.23) h after emergence of the primary germ tube; these were termed class D germinations (Fig. 2D; see Movie S2D in the supplemental material). The time interval ($e_2 - e_1$) between the emergence of the first and the second growing tip was significantly longer in class D germinations than in class B germinations (Table 1), although the length of arrest caused by branching (class A) or appearance of a second germ tube (class B) was not significantly different (Table 1). However, the time intervals between emergence of a primary and a secondary growth site were significantly longer when the second extending tip was derived from a branch (class A or C) rather than a germ tube (class B or D), irre-

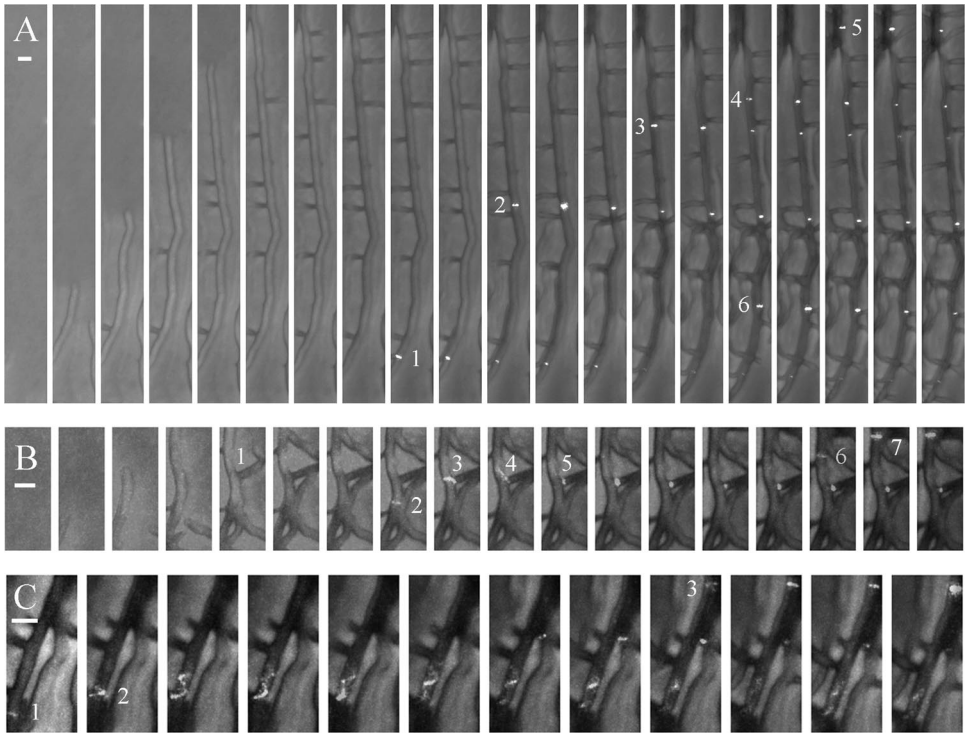

FIG. 3. Localization of FtsZ rings in growing *S. coelicolor* K113 substrate hyphae. Spores were germinated overnight before being transferred to an imaging chamber and allowed to equilibrate for 1 hour before commencement of imaging. The mosaic images are composed of images taken at 30-min intervals, while images taken at 15-min intervals are shown in Movies S3, S3A, S3B, and S3C in the supplemental material. Horizontal white bars represent 2 μm. (A) Hyphal branching and progression of FtsZ rings (1 to 6) toward the growing hyphal tip; it is not clear if FtsZ ring 6 is located in the primary hypha or a parallel hypha. (B) Progression (2 to 7) and division of an FtsZ ring (3) at a hyphal branch (1). (C) Extended FtsZ spiral (2) as FtsZ rings progress toward the hyphal tip (1 to 3).

spective of whether growth was arrested or not (Table 1). The timing of the initial germination had no effect either on the appearance of a second germ tube or on whether the primary germ tube underwent growth arrest (data not shown). Consequently, in a young *S. coelicolor* microcolony, and irrespective of whether one or two germ tubes emerge from a spore, if two young hyphal tips are located close to each other, one is able to exert an apical dominance over the other and arrest the latter's growth for a period of time.

FtsZ follows the extending hyphal tip and is not required for branching. *S. coelicolor* K113 spores failed to germinate when illuminated with light of a wavelength of 492 nm, which was necessary to excite EGFP. Despite this, we were able to visualize the movement of FtsZ-EGFP in substrate hyphae. K113 spores were inoculated onto 3MA as described previously and incubated overnight at 30°C. The next day, the cellophane square was transferred to an imaging chamber (Fig. 1), the tips of the radially extending mycelium identified by phase-contrast microscopy, and images captured as described above. This allowed us to visualize FtsZ-EGFP ring progression in growing substrate hyphae. Ten individual hyphae were observed with respect to their patterns of branching and Z-ring formation (see Movie S3 in the supplemental material). Hyphae grew across the field at an average tip extension rate of 19.58 (±2.67) μm h^{-1}, and branches formed on average 10.94 (±2.85) μm behind the hyphal tip. The average distance between branches was 7.63 (± 6.68) μm; this relatively large standard deviation associated with branch-to-branch distances suggests that *S. coelicolor* shows great variability in branch placement with respect to the location of other branches. These values were in broad agreement with those of Allan and Prosser (1). However, the relatively low standard deviation associated with the tip-to-branch distance suggests that branch placement is tightly linked to the distance from the hyphal tip. Taken together, the differences in the standard deviations of the tip-to-branch and branch-to-branch distances suggest that although *S. coelicolor* did not branch every time the tip-to-branch distance reached 10.94 μm, when it did so, the branch was placed close to 10.94 μm from the hyphal tip. A cessation of growth was seen in 82 (73.2%) branches that emerged from the 10 primary hyphae examined, while the remaining 30 branches (26.8%) displayed no growth arrest. It was apparent that when growth arrest occurred, the branch emerged in close proximity to a neighboring hypha (see Movie S3 in the supplemental material). In those branches where the tip displayed growth arrest, the tip-to-branch distance was significantly longer ($P < 0.02$), at 11.29 (±2.76) μm, than in those that displayed no growth arrest (10.06 [±2.93] μm). Rings of FtsZ-EGFP appeared at discrete locations after branching on average 56.06 (±16.96) μm behind the hyphal tip (Fig. 3A; see Movies S3 and S3A in the supplemental material) and presumably went on to initiate the formation of septa. Z rings formed on average 20.1 (±10.37) μm apart, and by measuring the distance between the apical and subapical Z rings and relating

this to the time difference between their appearances, we were able to calculate the rate of progression of the apical Z ring as 17.11 (±8.45) μm h^{-1}. Although rate of Z ring progression showed more variation than the rate of hyphal tip of extension (coefficients of variation were 51.6% and 13.6%, respectively), there was no significant difference between the two rates, which suggests either a direct or indirect association between Z-ring progression and peptidoglycan incorporation at the hyphal tip.

This reinforces the genetic evidence that FtsZ is not required for tip extension or branching in *S. coelicolor* (26), and although Z rings formed at some hyphal branch points (Fig. 3B; see Movies S3 and S3B in the supplemental material), this was not the case with many branches. Following the formation of a discrete Z ring, there was a transient increase in brightness of the ring (Fig. 3A; see Movies S3 and S3A in the supplemental material). The reason for this is unclear; perhaps it is due to movement of the ring out of the plane of the perpendicular, although a transient expansion of a compacted Z-ring spiral to produce apparent higher levels of fluorescence seems a more likely explanation. Z rings remained visible at the same location throughout the course of our observations, although many eventually faded to some degree. Occasionally, FtsZ spirals were seen (Fig. 3C; see Movies S3 and S3C in the supplemental material) and also moved toward the hyphal tip. Clearly the visible spiral displayed in Fig. 3C and in Movie S3C in the supplemental material moved much more slowly than Z-ring progression, and it took around 2 hours for the spiral to move through a 4-μm section of hyphae, before coalescing to form a discrete ring. The reason for this is not clear; although many other faintly fluorescing FtsZ spirals were observed distal to the apical Z ring (see Movie S3 in the supplemental material), suggesting that the progression of FtsZ behind the hyphal tip proceeds in a spiral manner.

Rehydration of aerial hyphae causes FtsZ-EGFP ring disassembly. *S. coelicolor* K113 was used to image the movement of Z rings by time-lapse microscopy in order to study the positioning and movement of FtsZ-EGFP in aerial hyphae. Coverslip-cellophane-grown cultures of *S. coelicolor* K113 were transferred to an imaging chamber, and aerial hyphae were identified by phase-contrast microscopy and subjected to time-lapse microscopy at 15-min intervals. In the absence of an agar plug, no further hyphal growth or development of aerial hyphae was seen, presumably due to hyphal dehydration or phototoxicity (data not shown). In order to maintain viability of aerial hyphae, it was necessary to apply a plug of tap water agar (Fig. 1). Despite this, the presence of tap water agar blocked the development of young aerial hyphae into spore chains and stimulated growth of substrate hyphae; we believe that the former was due to the premature disassembly of FtsZ-EGFP (Fig. 4; see Movie S4 in the supplemental material). If this is true, then it suggests that aerial hyphae have a means of sensing conditions inappropriate for sporulation and prevent its completion, either directly or indirectly, through the depolymerization of FtsZ-EGFP spirals. In older *S. coelicolor* K113 aerial hyphae, where there were no visible FtsZ-EGFP rings, presumably because they had already disassembled and initiated the laying down of divisional septa, is was possible for those aerial hyphae to complete the sporulation process and germinate (Fig. 5; see Movie S5 in the supplemental material).

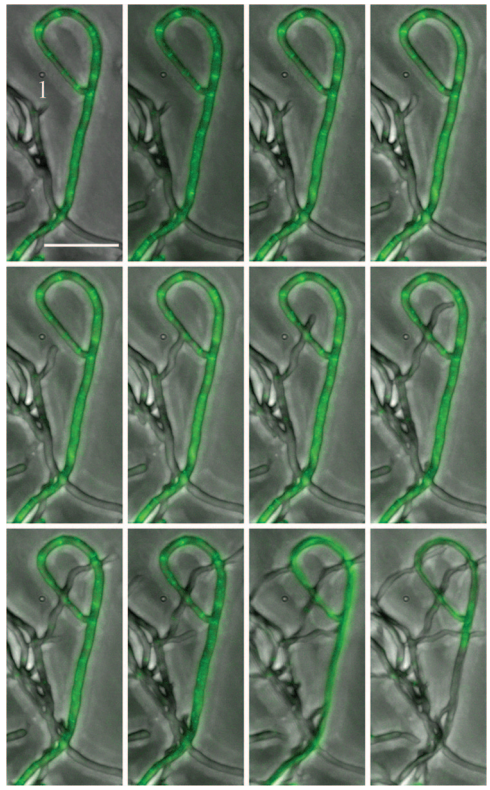

FIG. 4. Disassembly of FtsZ rings in aerial hyphae. Aerial hyphae of *S. coelicolor* K113 were grown on cellophane-covered coverslips for 36 h and transferred to imaging chambers. The mosaic image is composed of images taken at 30-min intervals, while Movie S4 in the supplemental material is composed of images taken at 15-min intervals. The horizontal white bar represents 10 μm. A hyphal tip activated for growth by transfer of the mycelium to the imaging chamber is labeled (1).

Septation, indicated by the regular invaginations, occurred simultaneously along the nascent spore chain proceeding through to the generation of mature spores that were subsequently able to undergo germination (Fig. 5; see Movie S5 in the supplemental material).

DISCUSSION

Time-lapse microscopy of *S. coelicolor* presents many challenges through its oxygen dependence, focal depth, mycelial heterogeneity, and agar-dependent sporulation. We have developed an imaging system allowing tracking of individual hyphae and proteins in conjunction with GFP that has overcome most of these difficulties through the use of an inverted microscope and agar plugs to flatten the mycelium as well as the provision of nutrients (13). Cellophane prevents hyphae from penetrating the agar plug and maintains the hyphae within a relatively narrow focal range, while the use of a motorized focus drive and the generation of Z sections means that phase-contrast images can be rendered in three dimensions to overcome the large focal depth required to image a mycelium. Finally, Ibidi μ-dishes allow the provision of oxygen to the mycelium.

In response to environmental and nutritional signals, *S.*

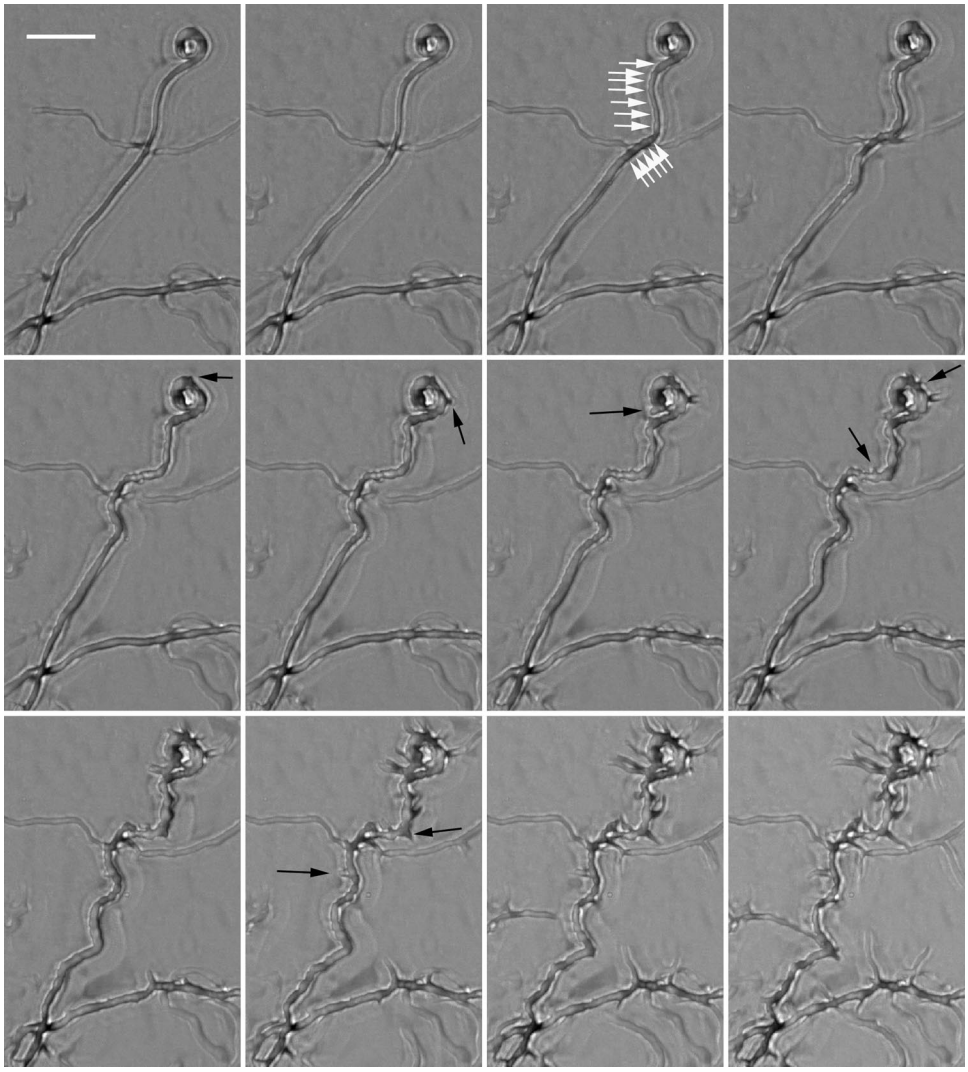

FIG. 5. Sporulation of *S. coelicolor* K113 aerial hyphae. Aerial hyphae of *S. coelicolor* K113 were grown on cellophane-covered coverslips for 36 h and transferred to imaging chambers. The mosaic image is composed of images taken at 30-min intervals while Movie S5 in the supplemental material is composed of images taken at 15-min intervals. The horizontal white bar represents 10 μm. White arrows show appearance of regular invaginations in the hyphal wall, characteristic of a forming spore chain. Black arrows show germinating spores.

coelicolor spores germinate following an initial increase in spore volume and differentiation of spore walls into an outer layer and an inner layer (14). The outer layer ruptures at the point(s) of germ tube emergence, while the inner layer forms the hyphal wall (27). The germ tube emerges to form an apical cell that grows by elongation through peptidoglycan synthesis, primarily at the hyphal tip (4, 6) but also to a lesser extent in subapical regions (9, 22), and is thought to be driven by hydrostatic pressure (23). The work reported here shows that if a second extension site develops close to the first, one of the extension sites is arrested for a period of time irrespective of whether the spore produces one or two germ tubes. The mechanism by which this arrest is achieved is not known; perhaps hyphal extension requires the presence of a nucleoid close to the tip and, as such, it is necessary for chromosome replication to take place before both tips possess an associated nucleoid and subsequently extend. Either chromosome replication or partitioning is associated with the earliest events of spore germination (12). Miguélez et al., (23) showed that in the presence of the peptidoglycan synthesis inhibitor vancomycin, DNA synthesis was arrested following the current round of replication, which suggests a close relationship between cell wall synthesis and chromosome replication. Even though Yang and Losick (30) were unable to find any evidence that DNA replication activity is concentrated at the apex, it seems likely that chromosome replication and segregation are linked with peptidoglycan incorporation, although the mechanisms by which this is achieved are unknown. The germinating spores of some *Streptomyces* species produce germination inhibitors (10) in order to inhibit extension of sibling germ tubes. It is thought that this provides a mechanism by which mass spore germination is prevented in order that potentially lethal mistakes in germination decisions are limited. *S. coelicolor* spores contain endogenous sources of nutrients such as trehalose (19, 20), and

it may be that growth arrest is a manifestation of a switch by the extending tip from an endogenous to an exogenous energy source or even a redeployment of nutrient resources within the microcolony. We were unable to generate movies of FtsZ-EGFP during germination, which is perhaps due to the inhibitory effects of light during spore germination seen in some streptomycete species (15). Following germination, hyphal extension occurred at a rate of ~20 μm h^{-1} and FtsZ-EGFP rings were laid down ~56 μm behind the growing tip. *Streptomyces granaticolor* lays down septa 28 μm from the hyphal tip (17), and as septum formation is dependent on the initial formation of a ring of FtsZ (26), it appears that either there is some variability in the frequency of septum formation between these two species or cultivation conditions affect septal frequency. It was thought that the subapical daughter compartment created a new extension site through branching (14) and this new apical cell was eventually partitioned from the subapical cell by a new septum. However, the movies presented here clearly show that branching occurs before rings of FtsZ-EGFP are laid down and septa form. While some branches do form FtsZ-EGFP rings at their bases, many do not. It may be that septa form at the bases of hyphal branches independently of FtsZ, but the movies presented here indicate that there is cytoplasmic continuity between many primary hyphae and their branches. Snapshot images of substrate hyphae stained with vancomycin-FL or FM4-64 show that many branches do not possess a septum at their base (data not shown). FtsZ-EGFP follows the extending hyphal tip at approximately the same speed (~20 μm h^{-1} in this system), which suggests that there is some form of association between the protein and extension site. Previous workers have shown that *ftsZ* mutants of *S. coelicolor*, although unable to sporulate, are able to support the growth and branching of substrate hyphae (7, 8, 21, 26). Both growth and branching of substrate hyphae occur before visible FtsZ-EGFP rings form, and it seems likely that the role of FtsZ in *S. coelicolor* substrate hyphae is to mark sites for septation. Perhaps the role of septa is to prevent cytoplasmic leakage in the event of a breach of the hyphal walls following a trauma such as phage lysis.

Although some streptomycetes can sporulate in liquid culture (14), the knowledge infrastructure available for *S. coelicolor* means that an imaging system capable of producing movies is essential for understanding the cell biology of this model organism. The system described here provides a means to do this to some degree. We were unable to image the erection of aerial hyphae and expect this to remain a recalcitrant problem due to repressive effects of the agar plug on the formation of aerial hyphae and the stimulatory effect on substrate hyphae following the transfer of coverslip-grown cultures to imaging chambers. Presumably the nutrients that supported growth of substrate hyphae in tap water agar came from action of the Dag protein that allows *S. coelicolor* to use agar as a nutrient source (2). Breaking of the surface tension by the action of SapB (29) is required for the erection of aerial hyphae by *S. coelicolor*, and it is not known whether aerial hyphae can be formed when they are trapped within the liquid phase; we have been unable to observe this. We believe that, as it was possible to image hyphae by phase-contrast microscopy, liquid from the agar plug permeated the cellophane and trapped any emerging aerial hyphae in the liquid phase. This prevented their further development and suggests that the ability of *S. coelicolor* to complete sporulation was dependent on the absence of hydration; if visible FtsZ-EGFP rings were seen in an aerial hypha at the time of their transfer to imaging chambers, hyphal maturation was blocked and FtsZ-EGFP rings disassembled (Fig. 4; see Movie S4 in the supplemental material). The simplest explanation for this is that aerial hyphae sense transfer from an aerial to a hydrated environment and signal FtsZ ring disassembly and developmental arrest. It is tempting to suggest that sensing of aerial growth may be through the sky pathway (3), where it is proposed that a signal molecule accumulates in the aerial hyphal wall and binds a sensor so that it can no longer diffuse into the medium and stimulates the expression of rodlin and chaplin genes. Perhaps, when aerial hyphae are transferred to an aqueous environment, diffusion of the signaling molecule not only prevents stimulation of *rdl* and *chp* expression, but also signals FtsZ ring disassembly. Despite this, in older hyphae, sporulation was able to proceed at least to the point where discrete, visible spores were visible (Fig. 5; see Movie S5 in the supplemental material), indicating the existence of point of no return beyond which sporulation cannot be blocked. Septation occurred simultaneously along the nascent spore chain, proceeding through to the generation of mature spores that were subsequently able to undergo germination (Fig. 5; see Movie S5 in the supplemental material). Understanding of this hyphal aging process, coupled with identification of the proteins that facilitate it, is essential to understanding the sequence of events during sporulation. In order to increase our understanding of the complex processes that underpin development of this complex bacterium, we will go on to refine this imaging system in order to "close the circle" with the aim of studying growth and protein trafficking during all stages of the *S. coelicolor* life cycle.

ACKNOWLEDGMENTS

This work was supported by BBSRC grant BB/D521657/1 and a University of Strathclyde Ph.D. studentship.

We are grateful to Klas Flärdh (Lund University, Sweden) for the provision of *S. coelicolor* K113. Helpful discussions with Nick Read (University of Edinburgh, United Kingdom) during development of the imaging system are gratefully acknowledged.

REFERENCES

1. **Allan, E. J., and J. I. Prosser.** 1983. Mycelial growth and branching of *Streptomyces coelicolor* A3(2) on solid medium. J. Gen. Microbiol. **129:**2029–2036.
2. **Bibb, M. J., G. H. Jones, R. Joseph, M. J. Buttner, and J. M. Ward.** 1987. The agarase gene (*dagA*) of *Streptomyces coelicolor* A3(2): affinity purification and characterization of the cloned gene product. J. Gen. Microbiol. **133:**2089–2096.
3. **Claessen, D., W. de Jong, L. Dijkhuizen, and H. A. B. Wösten.** 2006. Regulation of *Streptomyces* development: reach for ths sky! Trends Microbiol. **14:**313–319.
4. **Daniel, R. A., and J. Errington.** 2003. Control of cell morphogenesis in bacteria: two distinct ways to make a rod-shaped cell. Cell **113:**767–776.
5. **Elliot, M. A., M. J. Buttner, and J. R. Nodwell.** 2008. Multicellular development in *Streptomyces*, p. 419–438. *In* D. E. Whitworth (ed.), Myxobacteria: multicellularity and differentiation. ASM Press, Washington, DC.
6. **Flärdh, K.** 2003. Growth polarity and cell division in *Streptomyces*. Curr. Opin. Microbiol. **6:**564–571.
7. **Grantcharova, N., U. Lustig, and K. Flärdh.** 2005. Dynamics of FtsZ assembly during sporulation in *Streptomyces coelicolor* A3(2). J. Bacteriol. **187:**3227–3237.
8. **Grantcharova, N., W. Ubhayasekera, S. L. Mowbray, J. R. McCormick, and K. Flärdh.** 2003. A missense mutation in *ftsZ* differentially affects vegetative and developmentally controlled cell division in *Streptomyces coelicolor* A3(2). Mol. Microbiol. **47:**645–656.

9. **Gray, D. I., G. W. Gooday, and J. I. Prosser.** 1990. Apical hyphal extension in *Streptomyces coelicolor* A3(2). J. Gen. Microbiol. **136:**1077–1084.
10. **Grund, A. D., and J. C. Ensign.** 1985. Properties of the germination inhibitor of *Streptomyces viridochromogenes* spores. J. Gen. Microbiol. **131:**833–847.
11. **Han, L., A. Khetan, W.-S. Hu, and D. H. Sherman.** 1999. Time-lapsed confocal microscopy reveals temporal and spatial expression of the lysine ε-aminotransferase gene in *Streptomyces clavuligerus.* Mol. Microbiol. **34:** 878–886.
12. **Hardisson, C., M.-B. Manzanal, J.-A. Salas, and J.-E. Suàrez.** 1978. Fine structure, physiology and biochemistry of arthrospore germination in *Streptomyces antibioticus*. J. Gen. Microbiol. **105:**203–214.
13. **Hickey, P. C., D. J. Jacobson, N. D. Read, and N. L. Glass.** 2002. Live-cell imaging of vegetative hyphal fusion in *Neurospora crassa*. Fungal Genet. Biol. **37:**109–119.
14. **Hodgson, D. A.** 1992. Differentiation in actinomyctes. Soc. Gen. Microbiol. Symp. **47:**407–440.
15. **Imbert, M., and R. Blondeau.** 1999. Effect of light on germinating spores of *Streptomyces viridosporu*s. FEMS Microbiol. Lett. **181:**159–163.
16. **Kieser, T., M. J. Bibb, M. J. Buttner, K. F. Chater, and D. A. Hopwood.** 2000. Practical *Streptomyces* genetics. The John Innes Foundation, Norwich, United Kingdom.
17. **Kretschmer, S.** 1982. Dependence of the mycelial growth pattern of the individually regulated cell cycle in *Streptomyces granaticolor*. Z. Allg. Mikrobiol. **22:**335–347.
18. **Mazza, P., E. E. Noens, K. Schirner, N. Grantcharova, A. N. Mommaas, H. K. Koerten, G. Muth, K. Flärdh, G. P. van Wezel, and W. Wohlleben.** 2006. MreB of *Streptomyces coelicolor* is not essential for vegetative growth but is required for the integrity of aerial hyphae and spores. Mol. Microbiol. **60:**838–862.
19. **McBride, M. J., and J. C. Ensign.** 1987. Metabolism of endogenous trehalose by *Streptomyces griseus* spores or cells of other actinomycetes. J. Bacteriol. **169:**5002–5007.
20. **McBride, M. J., and J. C. Ensign.** 1990. Regulation of trehalose metabolism by *Sreptomyces griseus* spores. J. Bacteriol. **172:**3637–3643.
21. **McCormick, J. R., E. P. Su, A. Driks, and R. Losick.** 1994. Growth and viability of *Streptomyces coelicolor* mutant for the cell division gene *ftsZ*. Mol. Microbiol. **14:**243–254.
22. **Miguélez, E. M., C. Hardisson, and M. B. Manazanal.** 1993. Incorporation and fate of *N*-acetyl-D-glucosamine during hyphal growth in Streptomyces. J. Gen. Microbiol. **139:**1915–1920.
23. **Miguélez, E. M., C. Martín, M. B. Manazanal, and C. Hardisson.** 1992. Growth and morphogenesis in Streptomyces. FEMS Microbiol. Lett. **100:** 351–360.
24. **Noens, E. E., V. Mersinias, J. Willemse, B. A. Traag, E. Laing, K. F. Chater, C. P. Smith, H. K. Koerten, and G. P. van Wesel.** 2007. Loss of the controlled localization of growth stage-specific cell-wall synthesis pleiotropically affects developmental gene expression in an *ssgA* mutant of *Streptomyces coelicolor*. Mol. Microbiol. **64:**1244–1259.
25. **Reyes-Lamothe, R., C. Possoz, O. Danilova, and D. J. Sherratt.** 2008. Independent positioning and action of *Escherichia coli* replisomes in live cells. Cell **133:**90–102.
26. **Schwedock, J., J. R. McCormick, E. R. Angert, J. R. Nodwell, and R. Losick.** 1997. Assembly of the cell division protein FtsZ into ladder like structures in the aerial hyphae of *Streptomyces coelicolor*. Mol. Microbiol. **26:**847–858.
27. **Sharples, G. P., and S. T. Williams.** 1976. Fine structure of spore germination in actinomycetes. J. Gen. Microbiol. **96:**233–332.
28. **Van Keulen, G., J. Alderson, J. White, and R. G. Sawers.** 2007. The obligate aerobic actinomycte *Streptomyces coelicolor* A3(2) survives extended periods of anaerobic stress. Environ. Micobiol. **9:**3143–3149.
29. **Willey, J. M., A. Willems, S. Kodani, and J. R. Nodwell.** 2006. Morphogenetic surfactants and their role in the formation of aerial hyphae in Streptomyces coelicolor. Mol. Microbiol. **59:**731–742.
30. **Yang, M. C., and R. Losick.** 2001. Cytological evidence for association of the ends of the linear chromosome in *Streptomyces coelicolor*. J. Bacteriol. **183:** 5180–5186.